19.6 *Supernovae Observations and Classification*

The observation and classification of supernovae go back over 1000 years, making this one of the oldest branches of observational astronoy. The name "nova" had been given to "new stars" (actually outbursts from accreting white dwarfs), and "super"-novae were that much brighter. The names are similar in other cultures; e.g., Chinese records refer to them as *kexing*, or "guest stars."

Before the modern era began, there were $\sim$8 supernovae visible without telescopes. The brightest of these, SN 1006, is estimated to have had $m_V \approx -7.5$ mag, roughly 3 mag brighter than Venus and visible even in the daytime. Another famous example os SN 1054, whose ejecta now span a radius of $\approx$1.7 pc – this is the famous Crab Nebula[3] The two most famous, local (i.e., in the Milky Way) supernovae in "recent" times are Tycho's and Kepler's supernovae; these occurred "only" 30 years apart, in 1572 and 1604, and in Europe helped break down believes in a static, unchanging heavens and to unleash the modern astronomical revolution. No SN have been seen in the Milky Way since, although we think there should be 1–3 per year.

Like the classification of stars (discussed in Sec. 8), supernovae were classified into groups first and only later associated with underlying physical mechanisms. The observationally-motivated nomenclature comes from optical spectra of the supernova near peak luminosity (when it's easiest to observe), and it is:

- **Type I:** No H-α line seen.
- **Type II:** H-α line seen.

As simple as that! But this was subsequently clarified:

- **Type Ia:** No H-α, but Si lines seen.
- **Type Ib:** No H-α, but He lines seen.
- **Type Ic:** No H-α, and not much else.
- **Type II:** H-α line seen.

There are also multiple types of Type II supernovae, classified on the basis of their light curve morphology. E.g. SN1987A (lightcurve shown in in the rightmost panel of Fig. 41) was classified as Type IIpec, for "peculiar."

A **Type Ia supernova** is caused by fusion detonation on a degenerate white dwarf. Once the main source was thought to be mass transfer from a nearby binary companion onto the white dwarf, until the WD's degeneracy pressure can no longer support itself. But we now know that there are many pathways leading to SNe Ia; different pathways lead to different chemical abundances in the SN ejecta, and these studies now indicate that most SNe Ia (at least in dwarf galaxies) occur from white dwarfs of roughly $\sim 1 M_\odot$, well below the Chandrasekhar Mass of $1.4 M_\odot$. These SNe Ia are typically brighter — less

[3]Note that its ejecta have moved $\sim$5 light years over the past millenium, implying an *average* speed of 0.5% c – and presumably higher (and more relativistic) at earlier times.

total energy is released, but more of the energy here goes into photons rather than into neutrino luminosity.

Types II, Ib, and Ic are all different flavors of core-collapse supernovae probably resulting from progenitor stars with different initial masses and evolutionary histories.

In many supernovae, many of the photons we see actually come from the radioactive decay of unstable isotopes produced in the explosion. The most important pathway comes from the decay of ^{56}Ni, which was itself produced from fusion of Si with a succession of α particles:

(484) $^{28}_{14}\mathrm{Si} + 7^{4}_{2}\mathrm{He} \rightarrow^{56}_{28} \mathrm{Ni}$

or by direct, Si-Si fusion:

(485) $2^{28}_{14}\mathrm{Si} \rightarrow^{56}_{28} \mathrm{Ni}.$

The decay pathway after the supernova is over and nucleosynthesis has ceased is

(486)
$$^{56}\mathrm{Ni} \rightarrow^{56} \mathrm{Co} + e^{+} + \nu_e + \gamma \quad (6.1 \text{ day half} - \text{life})$$

(487)
$$^{56}\mathrm{Co} \rightarrow^{56} \mathrm{Fe} + e^{+} + \nu_e + \gamma \quad (78 \text{ day half} - \text{life})$$

(488)

Note that the ^{56}Co phase of SN1987A is indicated in Fig. 41. That SN was estimated to produce just $0.075 M_{\odot}$ of ^{56}Ni, but others produce as much as $\sim 1 M_{\odot}$ — these are extremely luminous.

20 Compact Objects

20.1 *Useful references*

- Prialnik, 2nd ed., Ch. 10
- Choudhuri, Secs. 5.3–5.6
- Hansen, Kawaler, and Trimble, Ch. 10

20.2 *Introduction*

As we have discussed up to this point, mass is destiny when describing the evolution and final fates of single stars. Fig. 43 breaks down the ultimate states of stars of a range of initial masses. Furthermore, the mass of an objects final remnant (after AGB mass loss, supernova, etc.) is similarly deterministic.

- $\mathbf{M_{fin}} < \mathbf{1.4 M_\odot}$: White dwarf, supported by electron degeneracy pressure.
- $\mathbf{1.4 M_\odot} < \mathbf{M_{fin}} \lesssim \mathbf{3 M_\odot}$: Neutron star, supported by neutron degeneracy pressure. The upper limit here is not known with great precision.
- $\mathbf{M_{fin}} \gtrsim \mathbf{3 M_\odot}$: No known support can hold up the remnant; it collapses into a gravitationally singularity, a **black hole.**

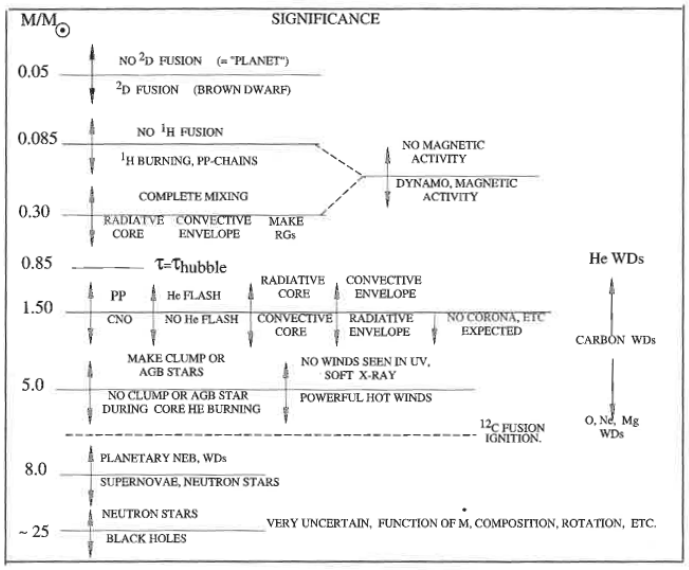

Figure 43: Mass is destiny: final fates of single stars. (Fig. 2.4 of Hansen, Kawaler, and Trible, 2nd Ed.).

Fig. 44 shows the masses of known stellar remnants, emphasizing that we know almost nothing about compact objects with masses between 2–5 $M_\odot$. But before we examine these most massive of remnants, let's first reconsider white dwarfs in a bit more detail.

20.3 *White Dwarfs Redux*

Let's construct a more detailed model of a white dwarf than what we've managed before. For example, we've talked before about the WD equation of state and qualitatively estimated their radii, but we can do better.

White dwarf mass-radius relations

Assume we have N electrons that supply the supporting degeneracy pressure, and N protons supplying the mass. Gravity packes the particles closely together (though not as tightly as in a neutron star!). By the Heisenberg uncertainty principle,

$$\Delta x \Delta p \gtrsim \hbar \tag{489}$$

the tight constraints on position imply a correspondingly large momentum dispersion, and so the total kinetic energy will increase.

So the Fermi momentum of the electrons will be approximately

$$p_F \approx \frac{\hbar}{\Delta x} \approx \hbar n^{1/3}. \tag{490}$$

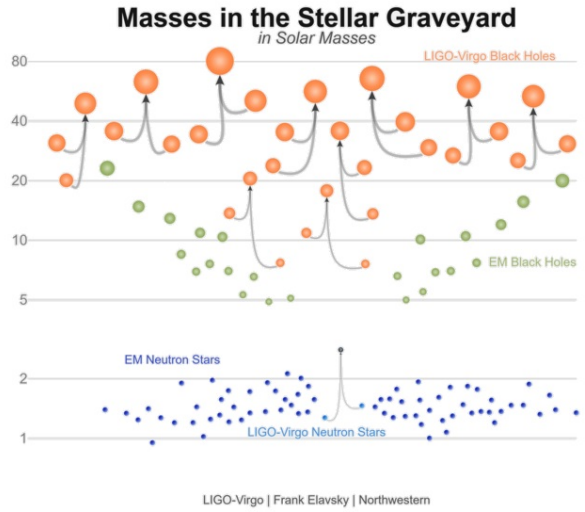

Figure 44: Masses of known extremely compact objects: black holes (above) and neutron stars (below), as of early 2019. Objects joined by arrows indicate mergers observed via gravitational waves.

And thus the total Fermi energy will be

$$E_F = \sqrt{p_F^2 c^2 + m_e^2 c^4}. \tag{491}$$

Depending on whether or not the electrons are strongly relativistic, we will have either

$$E_{F,NR} \approx m_e c^2 + \frac{p_F^2}{2m_e} \tag{492}$$

$$\approx C + \frac{\hbar^2}{2m_e}\left(\frac{N}{R^3}\right)^{2/3} \tag{493}$$

or

$$E_{F,UR} \approx p_F c \tag{494}$$

$$approx \frac{\hbar N^{1/3} c}{R}\left(\frac{N}{R^3}\right)^{2/3} \tag{495}$$

The total gravitational energy will be dominated by the more massive proton, and will be roughly

$$E_G \approx -\frac{GM^2}{R} = -N\frac{GMm_p}{R}. \tag{496}$$

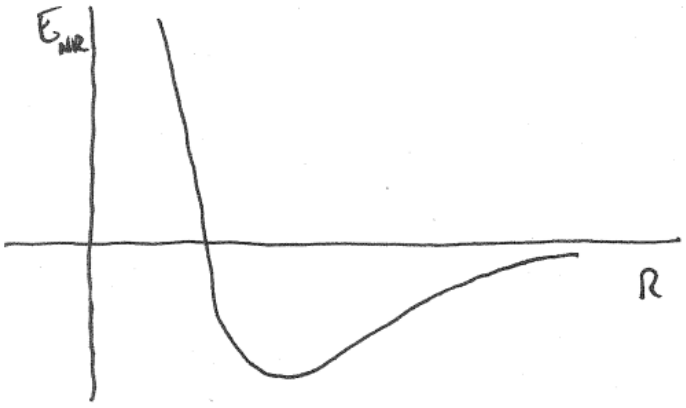

Figure 45: Total energy of a white dwarf in the non-relativistic limit (see Eq. 497). The energy minimum implies an equilibrium point: this will be the radius of the white dwarf.

Thus in the non-relativistic limit, the total energy of the system will be

$$E_{NR} \approx C + \frac{\hbar^2}{2m_e}\left(\frac{N^{5/3}}{R^2}\right) - \frac{GM^2}{R}. \tag{497}$$

This expression shows a clear minimum when plotted vs R (see Fig. 45) – this minimum is the equilibrium point, and corresponds to the radius at which a white dwarf is stable. This minimum radius occurs when

$$\frac{dE}{dR} = 0 \tag{498}$$

$$-\frac{\hbar^2 N^{5/3}}{m_e R^3} + \frac{GM^2}{R^2} = 0 \tag{499}$$

or equivalently, when

$$R = \frac{\hbar^2}{G m_e m_p^{5/3} M^{1/3}}. \tag{500}$$

Thus a typical white dwarf with mass $1M_\odot$ will have a radius of just about $1R_\oplus$. Furthermore, note that $R \propto M^{-1/3}$ – so white dwarfs get smaller as we add more mass, as we saw in Sec. 17.4. (We already encountered this while discussing shell burning: as fusion 'ash' is steadily added to a core, it contracts despite its mass having increased.)

Alternatively, in the ultra-relativistic case the total energy of the white dwarf will be

$$E_{UR} \approx \frac{\hbar c N^{4/3}}{R} - \frac{GM^2}{R} \tag{501}$$

$$= \frac{N^2}{R}\left(\hbar c N^{-2/3} - G m_p^2\right) \tag{502}$$

This expression, in contrast to Eq. 497, has no extremum with radius. So rather than a relation between mass and radius, a white dwarf in the ultra-relativistic has a single, limiting mass, given when $E = 0$:

$$\hbar c N^{-2/3} = G m_p^2. \tag{503}$$

This limiting mass is the aforementioned **Chandrasekhar Mass**, which is ap-

proximately

(504)

$$M_{Ch} \approx N_{max} m_p$$

(505)

$$\approx m_p \left(\frac{\hbar c}{G m_p^2} \right)^{3/2}$$

(506)

$$\approx 1.7 M_\odot$$

This is actually not too far off from what a further refinement would predict; we will consider this next.

Polytropic White Dwarf

The next level of refinement is to return to our polytropic model of a white dwarf, which we have discussed previously. As we've seen many times, for white dwarfs we have either

- **Non-relativistic degenerate gas**: $\gamma = 5/3, n = 3/2$.
- **Ultra-relativistic degenerate gas**: $\gamma = 4/3, n = 3$.

And as you just saw in Problem Set 7, the mass of a polytropic white dwarf is

(507) $$M = 4\pi \rho_c \lambda_n^3 \xi_{surf}^2 \frac{d\phi_n}{d\xi} \bigg|_{\xi_{surf}}$$

where

(508) $$\lambda_n \left[\frac{(n+1) K \rho_c^{1-n/n}}{4\pi G} \right]^{1/2}$$

and where ξ_{surf} is the Lane-Emden surface coordinate, introduced in Sec. 13.

This means that we have either

$M \propto \rho_c^{1/2}$ (for n=3/2), or

$M \propto \rho_c^0$ =const (for n=3)

and so the mass will steadily increase up to some maximum value, as shown in Fig. 46. To find the transition point and calculate the maximum mass, we need more details. Of particular import is the polytropic constant K_{UR}. The full equation of state turns out to be

(509) $$P = \left(\frac{3}{\pi} \right)^{1/3} \frac{hc}{8 m_p^{4/3}} \left(\frac{\rho}{\mu_e} \right)^{4/3}$$

which leads to a more accurate version of the Chanrasekhar Mass,

$$M_{Ch} = 1.4 M_\odot \left(\frac{\mu_e}{2}\right)^{-2}. \quad (510)$$

Observations of White Dwarfs

The observational history of white dwarfs is much messier – possibly even more complicated than solving polytropic equations of state. Observations established the existence of unusual celestial objects, but their natures weren't known for some time.

We now know that the first white dwarf was identified in 1783 by William Herschel. He noticed a dim companion to the $V = 4.4$ mag star 40 Eri. The colors of the faint companion indicated that it must be hot (we know now it's $\sim 10^4$ K, hotter than 40 Eri), but it is 5 mag fainter. Thus it must be tiny.

Another, similar object was identified four-score years later; this was Sirius B, discovered using a telescope in Cambridgeport, Massachusetts. Its gravitational connection to Sirius was quickly recognized, and using the tools discussed in Sec. 4.3 its mass, luminosity, and (after a "high-contrast" spectrum was obtained in 1915) its temperature were all measured. These indicated $M \approx M_\odot$, $T_{\rm eff} \approx 25,000$ K, and $R \approx 0.01 R_\odot$ — implying $\rho \approx 10^6$ g cm^{-3}.

These numbers were nonsense according to 19^{th} century astrophysics. Quantum mechanics was needed to understand such a bizarre object. It wasn't until 1926 that electron degeneracy pressure was described, and only in 1931 did Chandrasekhar identify his eponymous mass limit. Even so, conservative astronomers resisted for many years.

Other bibs and bobs about white dwarfs:

- As discussed in Sec. 17.7, the final composition of a white dwarf depends on its formation history. If it reached the 3α process, it should be carbon-oxygen. Otherwise, it's probably just a helium white dwarf. (There may be a chance to have O-Ne-Mg WDs, but there's no strong empirical evidence.)

- Some white dwarfs pulsate, permitting asteroseismlogy to more precisely determine their interior structure from the Fourier spectrum of oscillation modes.

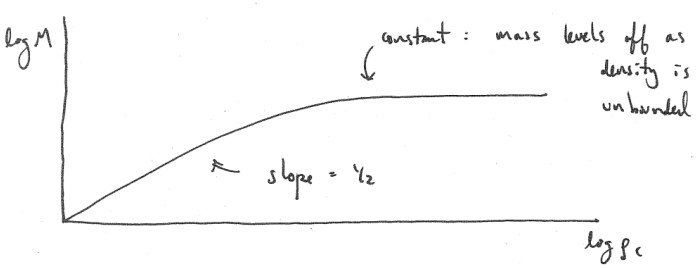

Figure 46: Mass of a white dwarf as its central density increases.

- Gravitational redshifts have been measured from some stars. Since a photon's energy as it leaves a gravitational well changes by

  $$\Delta E = h\nu \Delta\Phi_g / c^2 = h\nu \frac{GM}{c^2}\left(\frac{1}{\infty} - \frac{1}{R_{WD}}\right) \tag{511}$$

  one can measure the wavelength/frequency/energy of a known line relative to its expected location

  $$\frac{\Delta E}{E} = -\frac{GM_{WD}}{R_{WD}c^2} \tag{512}$$

  and so directly measure the WD's mass-to-radius ratio.

- As has been alluded to before, white dwarfs gradually cool down on cosmic timescales. By modeling this, we can estimate the ages of individual (isolated) WDs and also of star clusters. WDs in globular clusters provided one of the first signs that the universe was >10 Gyr old!

20.4 *White Dwarf Cooling Models*

White dwarfs start out extremely hot as the cores of giant stars, but once the stellar envelope is ejected they cool down: first rapidly, then slowly.

White Dwarfs: The Simple Model

In the simplest model of white dwarf cooling, the WD is an isothermal object radiating at temperature T, and its total internal energy is the kinetic energy of its constituent particles. Thus the total energy available to the WD is

$$E_{tot} \approx NkT = \frac{M}{m_p}kT \tag{513}$$

and its luminosity is

$$L = -\frac{dE_{tot}}{dt} = 4\pi R^2 \sigma T^4. \tag{514}$$

Since the white dwarf is degenerate we will assume that its radius is constant throughout its evolution. Then we have

$$-\frac{M}{m_p}k\frac{dT}{dt} = 4\pi R^2 \sigma T^4 \tag{515}$$

which, after some algebraic manipulation, yields

$$-T^{-4}dT = \frac{4\pi R^2 \sigma m_p}{Mk}dt \tag{516}$$